High Efficient Removal of Methylene Blue Using Microcrystalline Cellulose/Polyvinyl Alcohol/Expanded Graphite 3D Porous Foam as a “Green” Adsorbent

Xiaodong Tan (xiaodong.tan@tul.cz)
Technical University of Liberec https://orcid.org/0000-0002-8940-0160
Qingyan Peng
Technical University of Liberec: Technicka Univerzita v Liberci
Tereza Subrova
Technical University of Liberec: Technicka Univerzita v Liberci
Jana Saskova
Technical University of Liberec: Technicka Univerzita v Liberci
Jakub Wiener
Technical University of Liberec: Technicka Univerzita v Liberci
Mohanapriya Venkataraman
Technical University of Liberec: Technicka Univerzita v Liberci
jiri Militky
Technical University of Liberec: Technicka Univerzita v Liberci
Wei Xiong
Wuhan Textile University - Yangguang Campus: Wuhan Textile University
Jie Xu
Wuhan Textile University - Yangguang Campus: Wuhan Textile University
Arunjunai Raj Mahendran
Wood K plus
Herfried Lammer
Wood K plus

Research Article

Keywords: Cellulose, Polyvinyl Alcohol, Expanded Graphite, Foam, Methylene blue, Adsorption

Posted Date: March 25th, 2022

DOI: https://doi.org/10.21203/rs.3.rs-1421874/v1

Abstract

The cellulose/polyvinyl alcohol (PVA)/expanded graphite (EG) 3D porous foam, which has wide application prospects in cost-effective dye removal, was prepared by physical crosslinking and foaming technology. The prepared foam material has an obvious 3D network and porous structure, exhibiting excellent removal efficiency for methylene blue (MB) in an aqueous solution. The largest MB adsorption capacity of the foam is 110.81 mg/g. The adsorption process follows the pseudo-2nd order kinetics and the Freundlich isotherm model, indicating that the adsorption process is controlled by active surface sites and the physical adsorption process. Thermodynamic studies have shown that the adsorption process is a spontaneous and exothermic reaction. After five cycles of adsorption experiments, the composite material still exhibited a more than 70% dye removal rate. The results show that cellulose/PVA/EG 3D porous foam is effective, promising, and recyclable adsorbent, which can be used to remove MB from aqueous solutions.

1. Introduction

Dyes are widely used in the dyeing process of textiles, papermaking, pharmaceuticals, food, and other fields (Yang et al. 2021; Radwan et al. 2021). A large amount of the wastewater containing organics, which are often toxic, stable in aqueous solution, and difficult for natural degradation, are inevitably produced during the process of dyeing (Li et al. 2019; Bhatti et al. 2020). Methylene blue (MB) is a cationic dye widely used for testing of waste water treatment. At the same time, MB has a huge negative impact on the human body, such as meningitis, neuronal cell apoptosis, nausea, and vomiting (Oz et al. 2011). Many methods have already been applied in solving wastewater, such as membrane filtration, flocculation, co-precipitation, chemical redox, and biological treatment (Jiang et al. 2018; Ge et al. 2018; Liu et al. 2019; Usmani et al. 2021). However, these methods have some restricting factors in their application, such as high cost, unfavorable recycling, and secondary pollution.

Adsorption is a common method to sequester organic dyes from wastewater (Azha et al. 2017). Compared with other methods, the adsorption shows low cost, high efficiency, easy recovery, and high selectivity (Bhatti et al. 2018). Some traditional adsorbents have been widely discussed. Mahdi Hasanzadeh et al. developed an activated carbon/metal-organic framework composite material to obtain extremely high adsorption capacity in the removal of anionic dyes, and the adsorption process performs the Langmuir model, which indicates chemical adsorption (Hasanzadeh et al. 2020). Lamia Dali Youcef et al. studied the performance of a zeolite in adsorbing cationic dyes. Studies have shown that an excellent dye removal rate can be obtained at a lower dye concentration (Dali Youcef et al. 2019). Zhihui Huang et al. studied modified bentonite to adsorb Rhodamine B and Acid Red 1. It was found that the maximum adsorption capacity of Rhodamine B and Acid Red 1 were 173.5 mg/g and 157.4 mg/g, respectively (Huang et al. 2017). Although these traditional adsorbents are popular, they have poor regeneration ability and are toxic to many organisms. Meanwhile, these adsorbents, based on chemical adsorption during the adsorption process, are hardly reused (Al-Ghouti and Al-Absi 2020).

Based on the requirements of environment-friendly adsorption, biosorbents have received extensive attention. Among them, cellulose and polyvinyl alcohol (PVA) are widely used as biosorbents due to outstanding characteristics such as low cost, solubility, good mechanical strength, stability, biocompatibility, and non-toxicity (Li et al. 2012). Expanded graphite (EG) is a common carbon material. Compared with graphene, carbon nanotube and graphene oxide have many advantages, such as huge porosity, excellent chemical properties, thermal stability and good mechanical stability, which have significant superiority in adsorption (Hu et al. 2019; Verma et al. 2020).

As porous materials have been developed rapidly in recent decades, related research is focused on aerogels and hydrogels. 3D network materials with open porous and microporous structures show great potential in wastewater adsorption (Franco et al. 2021). Sheng Tang et al. developed an amphiphilic graphene aerogel for the adsorption of dyes and found the best effect on the adsorption of malachite green (Tang et al. 2019). Shu Wang et al. prepared a silk fibroin-modified graphene oxide-based aerogel, which showed excellent adsorption capacity in methylene blue (Wang et al. 2019). However, some problems of studied porous materials include expensive raw materials, costly manufacturing, and complicated drying process (Karami 2018; Asim et al. 2019).

Foam materials also have an open porous structure, convenient preparation process, and extremely low production cost for wider use (Lu et al. 2021). The trimethylammonium grafted cellulose foam prepared by Chuting Feng et al. can selectively adsorb anionic dyes and obtain better adsorption performance (Feng et al. 2020). Hong Ma et al. developed flexible cellulose foam to obtain high adsorption capacity(116 mg/g) (Ma et al. 2021).

In this work, we prepared the cellulose/PVA/EG 3D porous foam by developing a simple and feasible strategy for the removal of methylene blue. After simple foaming and solidification, the prepared foam has a stable 3D and open porous structure, which can efficiently and cyclically remove methylene blue and has broad application in dye wastewater treatment.

2. Experiment

2.1 Materials

Microcrystalline cellulose (MCC, 98%, 20μm), PVA (molecular weight 72000), Sodium dodecyl sulfate (SDS, 99%), Sodium hydroxide (NaOH), Polyethylene glycol 4000 (PEG), MB, and Ethanol were supplied by Sigma Aldrich (ST. Louis, USA). EG was provided by the Technical University of Liberec. All the solutions used distilled water with 18 MΩ cm electrical resistivity.

2.2 Preparation of Cellulose Solution in PEG + NaOH System

The procedure of cellulose solution was carried out according to the method reported by Yan and Cernencu et al. (Yan Zhijuan Gao; Cernencu et al. 2017). At first, 2wt% PEG and 9wt% NaOH were

dissolved in 40 ml of distilled water. Then, 2wt% MCC was added to this solution, continuously stirring for 3h. Finally, the suspension was frozen at -20℃ for 12h and then thawed at room temperature. This step was repeated three times.

2.3 Preparation of 3D Porous Foam Material

At first, 10wt% PVA and 5wt% EG were added into the suspension with stirring at 600 rpm and 85℃ for 3h. Then 2wt% SDS was added with stirring for 30min to emulsify and foam the suspension. At last, the suspension was frozen for solidification at -20℃ for 72h. After thawing, the porous foam material was obtained (Fig. S1). Herein, samples were named according to the composition of the added chemicals, such as PVA + SDS (PS), MCC + PVA (CP), MCC + PVA + SDS (CPS), and MCC + PVA + SDS + EG (CPSG).

2.4 Morphology Test of Different Composites

The surface morphology of porous foam material was observed by Scanning electron microscope (SEM) (VEGA TESCAN Inc., USA)(Tan et al. 2021).

2.5 Adsorption Experiment of MB

For the adsorption experiment, MB was chosen as a model dye to check the adsorption property of porous foam materials. In short, different concentration solutions of MB were prepared by dilution for construction of the calibration curve (Fig. S2).

Then, we put 0.06g sample into 30 ml different concentration solution of MB (25 mg/L, 50 mg/L, 100 mg/L, 150 mg/L, 200 mg/L, 250 mg/L). UV-spectrophotometer (7415, Cole-Parmer Ltd.) was utilized to determine the concentration of residual MB dye in the solution after adsorption at 665 nm wavelength. The dye removal efficiency and adsorption capacity were calculated according to Eq. 1 and Eq. 2 (Wang et al. 2018).

$$Removalpercentage(R\%) = \frac{C_0 - C_t}{C_0} \times 100\%$$

1

$$Adsorptioncapacity\left(q_t\right) = \frac{(C_0 - C_t) \times V}{m} \times 100\%$$

2

Where C_0, C_t (mg/L) are the concentrations of MB at zero time and time *t*, respectively. V is the MB solution volume (L) and m (g) is the mass of the sample.

2.6 Recycling Test

The sample containing adsorbed MB was placed into absolute ethanol solution for 72h at room temperature. Then, the adsorption experiment was repeated after most MB was desorbed from samples.

3. Results

3.1 Surface Morphology of Different Structures

As we can see from Fig. 1a ~ d, it can be clearly observed that CPS and CPSG have a 3D porous structure. In contrast, PS only forms a 2D film, and CP forms a 3D structure without porous structure. At first, as a water-soluble, soft, and long-chain polymer, PVA has widely been applied in the preparation of permeable membrane, aerogel, and hydrogel due to its excellent film-forming and excellent chemical properties (Sonker et al. 2018). However, even if we added any foaming agent in this research, there was still no porous structure. This may be because we utilized freezing instead of freeze-drying in this experiment. So, in the subsequent thaw process, its 3D structure collapsed. In addition, bubbles generated by the foaming agent could not form porous structure in the final solidification due to the collapse of the overall structure.

In contrast to CP, CPS and CPSG formed a good 3D structure. The main reason is the addition of cellulose. It is well-known that cellulose consists of a well-organized crystallinity region that contributes to the strength, high stiffness, and amorphous region, which makes fiber more flexible (Kalia et al. 2011; Lavoine et al. 2012). Cellulose is added to the system as a reinforcing component filler, forming a uniform network and stable 3D structure in the mixed solution with PVA through hydrogen bonding and supramolecular interaction. Song et al. prepared a cellulose-PVA hydrogel material. They found that after adding cellulose, the mechanical strength of the composite material was significantly enhanced, and the structural stability of the material was improved (Song et al. 2020).

Foam molding technology has developed quickly in the past few decades. As an anionic surfactant, SDS has been widely used to foam cellulosic suspensions (Alimadadi and Uesaka 2016; Hou and Wang 2017; Viitala et al. 2020). Lee et al. successfully prepared porous 3D cellulose foam using 3D printing and foaming technology, with good mechanical properties and interesting structure (Lee et al. 2021). In this research, cellulose/PVA/EG 3D porous foam was physically cross-linked. Then the PEG and SDS were washed away in the subsequent washing process (Fig. S4) and initially utilized SDS as a foaming agent and surfactant to prepare foam material. Compared with CPS and CPSG, SDS is the key to porous forming. Foam is a complex gas/liquid dispersion system. In the effect of high shear force, massive bubbles are generated and accumulated in a trace amount of surfactant solution to form a liquid foam slurry (Weaire and Phelan 1996). As shown in Fig. 1g, those irregular bubbles fix the cellulose and EG particles between the gas and liquid phases (Hjelt et al. 2011). In addition, the liquid foam can be prepared by rearranging SDS molecules at the surface of air bubbles entrapped in a suspension (Liu et al. 2018). The hydrophobic area of SDS extends out of the bubble surface, and the hydrophilic area combines with water to form a surfactant layer. The negative charge of cellulose and EG caused electrostatic repulsion with SDS. So, they are repelled between the bubbles to form a water layer containing cellulose and EG. Although it has the same charge as cellulose and EG, they still adsorb to hydrophobic sites to form aggregates as SDS is a strong surfactant(Tucker et al. 2012).

3.2 Influence of Different Factors on Adsorption Performance

Adsorption is a surface phenomenon in which the solid surface of the adsorbent is bonded by adsorptive molecules (gas/liquid/solid phase). The whole adsorption process is mainly divided into three steps: (1) Film diffusion is also called external diffusion, in which the adsorbate is transported to the external surface of the adsorbent in the space; (2) Intraparticle diffusion (IPD), means that the adsorbate diffuses from the external surface of the adsorbent into the pores; (3) Surface reaction, means that the adsorbate is adsorbed on the inner surface of the adsorbent (Ho et al. 2000; Tan and Hameed 2017). In this case, the mass transfer effect needs to be considered. In the adsorption process, the first two steps are mass transfer, and the last step is the reaction step. The adsorption efficiency is determined by the adsorption resistance. Any step of the adsorption resistance in the above steps will have a huge impact on the total adsorption efficiency (Amanullah et al. 2000).

At first, transmission resistance is affected by many factors, including the type and structure of the adsorbent. We investigated the adsorption performance of different samples at relatively lower dye concentrations (25 mg/L). As seen in Fig. 2a, CPSG has the highest removal rate of dye (96.21%) and adsorption capacity (12.03 mg/g) compared to CP (16.51%, 2.06 mg/g) and CPS (65.02%, 8.13 mg/g). This is mainly due to the porous structure of CPSG, and MB molecules easily diffuse from the external surface to the internal surface. Moreover, EG provides more active sites and significantly improves the adsorption performance.

In addition, the effect of different initial dye concentrations (25 mg/L – 250 mg/L) on the adsorption performance was investigated. It can be seen from Fig. 2b that as the initial dye concentration increases, the adsorption capacity increases significantly from 12.03 mg/g to 110.81 mg/g, which is possibly caused by concentration polarization. At higher dye concentration, concentration polarization accelerates the diffusion rate of MB molecules on the surface of the adsorbent, and more dye molecules are adsorbed (Eltaweil et al. 2020a).

The pH value is also one of the important factors influencing adsorption performance. The research results show that the removal rate and adsorption capacity of MB increase with the increase of pH value, which is consistent with the relative researches (Fig. 2c) (Wang et al. 2018; Abd-Elhamid et al. 2019; Eltaweil et al. 2020a). At low pH, due to protonation, the positive charge on the surface of the material increases, which causes repulsion between cationic dyes and positively composite, resulting in low adsorption efficiency (Premarathna et al. 2019).

Moreover, the influence of different temperatures on the adsorption performance was investigated. It can be seen from Fig. 2d that as the temperature increases, the dye removal rate and adsorption capacity of the adsorbent decrease significantly, indicating that temperature is also an important influencing factor of the adsorption performance. As the temperature increases, the thermal mobility of dye molecules increases, which may accelerate their transport to the surface of the adsorbent. However, at the same

time, it may also accelerate the desorption of dye molecules from the surface of the adsorbent (Sabarish and Unnikrishnan 2018).

3.3 Adsorption Kinetic of Adsorbent in MB

There are two possible interactions between adsorbate and adsorbent, namely chemical and physical interaction. Among them, chemical interaction is also called chemical adsorption in that there are chemical or covalent bonds between adsorbate and adsorbent by sharing or transferring electrons. On the other hand, the main force that dominates physical adsorption are van der Waals forces mainly(Dąbrowski 2001).

It is very important to figure out whether an adsorption phenomenon is a chemical or physical adsorption, which can help us understand its adsorption mechanism. Adsorption kinetics reveals the relationship between adsorption efficiency and time and is a good tool to analyze the adsorption rate. This research chooses the three most commonly used kinetic models (Pseudo-1st order, Pseudo-2nd order and IPD model) to study the adsorption rate. The equation of Linearized form is shown in Table S1.

Batch adsorption experiments were performed with different concentrations of dye solutions at 25 ℃, and the samples were tested every 30 minutes. The adsorption kinetics curves and parameters are shown in Fig. 3 and Table 1. It is obvious that the Pseudo-2nd order is more suitable than the Pseudo-1st order. It reveals that the adsorption process depends on the number of active sites (Wang and Guo 2020a).

However, some research has reported that the kinetic data near equilibrium may have serious deviations if a Pseudo-2nd order kinetic model is applied (Simonin 2016). Therefore, other models are needed for further study on the adsorption rate.

The IPD model is used to determine the rate-limiting steps of the entire adsorption process. As shown in Fig. 3c and Table 1, $k_{i-1stage} > k_{i-2stage} > k_{i-3stage}$ indicates changes in diffusion rate, revealing that the adsorption process mainly follows three steps: (1) The first stage is the diffusion of MB molecules from the body to the external surface of the adsorbent; (2) Then, MB molecules diffuse through the pores and diffuse into the internal surface; (3) The last stage is near equilibrium stage. In this stage, the balance of adsorption and desorption is reached.

Table 1
Parameters of adsorption kinetic

Models	Parameters	25 mg/L	50mg/L	100 mg/L	150 mg/L	200 mg/L	250 mg/L
Pseudo-1st order	$q_{e,exp}$(mg/L)	12.03	24.91	48.94	73.49	90.90	110.81
	$q_{e,cal}$(mg/L)	4.49	5.55	12.40	15.92	42.84	98.50
	$k_1(min^{-1})$	-0.8963	-0.8271	-0.4998	-0.4887	-0.5565	-1.083
	R^2	0.902	0.741	0.688	0.629	0.888	0.944
Pseudo-2nd order	$q_{e,exp}$(mg/L)	12.03	24.91	48.94	73.49	90.90	110.81
	$q_{e,cal}$(mg/L)	12.56	25.06	48.19	72.20	92.17	123.03
	$k_2(min^{-1})$	0.4240	0.6130	0.2210	0.2014	0.0370	0.0161
	R^2	0.999	0.999	0.999	0.999	0.998	0.998
IPD 1 Stage	k_i	1.86	3.64	10.07	13.97	17.00	63.95
	C	20.77	6.84	33.72	53.03	54.24	16.26
	R^2	0.998	0.976	0.872	0.911	0.768	0.992
IPD 2 Stage	k_i	0.85	1.16	3.53	3.26	14.08	25.81
	C	22.95	9.76	40.59	64.94	57.40	60.64
	R^2	0.715	0.939	0.915	0.912	0.797	0.649
IPD 3 Stage	k_i	0.72	1.02	1.36	2.61	13.33	8.17
	C	23.01	9.89	44.31	65.49	58.29	93.19
	R^2	0.986	0.882	0.984	0.878	0.941	0.999

3.4 Adsorption Isotherm of Adsorbent in MB

The adsorption isotherm is to study the relationship between the concentration of adsorbate in the liquid phase and the adsorbent at a specific temperature at equilibrium. Modeling the equilibrium adsorption data can help us study the adsorption mechanism, the interaction between the adsorbate and the adsorbent, the maximum adsorption capacity, and so on (Wang and Guo 2020b). In this study, several models (Langmuir, Freundlich and Temkin) were selected to analyze the adsorption mechanism (Table S2).

It can be seen from Fig. 4 and Table 2 that the Freundlich model (R^2 = 0.954, 0.991, 0.979) is more suitable than Langmuir (R^2 = 0.983, 0.863, 0.771) and Temkin model (R^2 = 0.935, 0.871, 0.919) for describing the adsorption of MB molecules on cellulose/PVA/EG porous materials. It reveals the multilayer adsorption of MB on heterogeneous surfaces. Multilayer adsorption is due to mutual attraction between molecules, and additional molecules are superimposed on the first adsorption layer to form multilayer adsorption, which is essentially physical adsorption. In addition, n represents the adsorption strength of the adsorbent. When $n > 1$, it indicates that the adsorption behavior is favorable (Eltaweil et al. 2020a). At the same time, porous adsorbent has a greater adsorption strength at 25 ℃ as the lowest temperature in the test, indicating that high temperature is unfavorable for the adsorption behavior, which further supports its physical adsorption behavior.

Table 2
Key parameters of adsorption isotherm model

	Langmuir			Freundlich			Temkin		
	q_m (mg/g)	b (L/mg)	R^2	k_f (L/mg)	n	R^2	B_1 ($Jmol^{-1}$)	A (L/mg)	R^2
25 ℃	112.38	0.5161	0.983	43.1121	3.516	0.954	16.12	21.4108	0.935
50℃	30.30	0.0113	0.863	13.2766	2.1404	0.991	18.06	1.5371	0.871
75℃	70.72	0.0048	0.771	9.8355	2.4114	0.979	13.19	1.0879	0.919

3.5 Thermodynamic of Adsorption

Adsorption thermodynamic is used to survey the trend, degree, and driving force of the adsorption process and plays an important role in explaining the characteristics, laws, and mechanism of adsorption. The changes of parameters of thermodynamic of the adsorption process are generally calculated by equations of Gibbs equation and Vant' Hoffs (Lakouraj et al. 2015):

$$\Delta G = -RTlnK_c \quad (3)$$

$$K_c = \frac{q_e}{C_e} \quad (4)$$

$$lnK_c = \frac{\Delta S}{R} - \frac{\Delta H}{T} \quad (5)$$

Where ΔG (kJ/mol) is Gibbs Free Energy, R and T are gas constant (8.314 J/mol/K) and absolute temperature (K), K_c (L/mol) is the equilibrium constant of adsorption, ΔS and ΔH are entropy and enthalpy, respectively.

As shown in Table 3, the free energy ΔG is negative, indicating that the porous material adsorbs MB as a spontaneous process. As the temperature increases, the absolute value of ΔG decreases, indicating that the spontaneous tendency of adsorption decreases, which is not conducive to adsorption. The negative value of the adsorption enthalpy ΔH reveals that the adsorption process is an exothermic reaction. The negative value of the adsorption entropy ΔS indicates that the adsorption reduces the degree of freedom of the adsorbate molecules.

Table 3
Parameters of the thermodynamic model

	ΔG (kJ/mol)	ΔH (kJ/mol)	ΔS (kJ/mol/K)
25 ℃	-7.9121	-55.7537	-0.1622
50℃	-2.0405		
75℃	-0.0663		

3.6 Reusability of the adsorbent

For industrial applications, the regeneration and recycling of adsorbents are very important. In this study, the adsorbent after adsorption was immersed in an ethanol solution to regenerate it. The experimental result shows that after five cycles, the MB dye removal rate of the composite material drops from 97.98–71.93%, possibly for a combination of chemistry and physics adsorption of cellulose/PVA/EG foam (Fig. 5). As is known to all, chemical adsorption is irreversible, but physical adsorption is reversible. Therefore, the adsorption process was mainly led by physical adsorption in the subsequent cycle. To sum up, the removal rate of adsorbents after regeneration remains high, which is appropriate for the treatment of MB wastewater.

3.7 Adsorption mechanism of Cellulose/PVA/EG Foam in MB

The adsorption mechanism of the adsorbate on the adsorbent is affected by many factors, such as the size and structure of the adsorbent. Based on the above experimental results, the adsorption mechanism scheme lists in Fig. 6. According to analyzing adsorption kinetics and isotherm, the adsorption process is mainly physical adsorption affected by the number of active sites and adsorbent structure. So, the possible interactions that determine the effect of MB adsorption are electrostatic adsorption, hydrogen bonding, and van der Waals force.

3.8 Comparison to other adsorbents of Adsorption Performance in MB

As shown in Table 4, the adsorbent has significant advantages. The main components of the materials are cellulose, PVA, and EG. These materials are low-cost, renewable, easy to recycle, and degraded. Although the materials developed by Boukhalfa, N., and Eltaweil, A.S. et al. have high adsorption capacity (Boukhalfa et al. 2019; Eltaweil et al. 2020b), the cost of their adsorption materials, such as carbon nanotubes or graphene oxide, is very high.

Table 4
Adsorption performance of different adsorbents on MB molecules

Adsorbent	Concentration of MB	Removal percentage (%)	q_e (mg/g)	Ref.
Cellulose based porous foam composites	250 mg/L	90.9	110.8	This research
Maghemite/alginate/functionalized multiwalled carbon nanotubes	230 mg/L	-	905.5	(Boukhalfa et al. 2019)
CMC/GOCOOH composite microbeads	250 mg/L	72.09	180.32	(Eltaweil et al. 2020b)
CMC-Alg/GO hydrogel beads	15 mg/L	96.2	78.5	(Allouss et al. 2019)
Salecan-g-PAI	500 mg/L	22.1	107.1	(Qi et al. 2018)
Magnetic chitosan/clay beads	100 mg/L	-	82	(Bée et al. 2017)
activated carbon/cellulose biocomposite films	100 mg/L	-	103.66	(Somsesta et al. 2020)

4. Conclusion

In this study, cellulose/PVA/EG 3D porous foam material was prepared by a simple foaming technique using physical crosslinking, and it was evaluated as a “green” and efficient adsorption material. Results show that cellulose strongly supports the 3D network structure of the material, and SDS effectively promotes the formation of the porous structure. The addition of EG significantly improves the removal efficiency of methylene blue. In the adsorption experiment, the dye concentration, pH, and temperature significantly affect the adsorption result of the material. The adsorption capacity is directly proportional to dye concentration and pH, while the adsorption capacity is inversely proportional to temperature. The adsorption process follows the pseudo-2nd order kinetics and Freundlich isotherm model. Thermodynamic studies have shown that the adsorption process is a spontaneous and exothermic reaction. In addition, after five cycles of adsorption, the repeatability study found that the dye removal rate remained high, although the adsorption capacity of the material decreased slightly. Therefore, the

prepared cellulose/PVA/EG 3D porous foam material is a stable, environmentally friendly, efficient, and reusable adsorbent for methylene blue removal.

Declarations

Acknowledgments

This work was supported by the Ministry of Education, Youth and Sports of the Czech Republic and the European Union-European Structural and Investment Funds in the Frames of Operational Programme Research, Development and Education-project Hybrid Materials for Hierarchical Structures(HyHi, Reg. No. CZ.02.1.01/0.0/0.0/16_019/0000843),

Declaration of Competing Interest

We have no known competing financial interests or personal relationships that could have appeared to influence the work reported in this paper.

References

1. Abd-Elhamid AI, Kamoun EA, El-Shanshory AA et al (2019) Evaluation of graphene oxide-activated carbon as effective composite adsorbent toward the removal of cationic dyes: Composite preparation, characterization and adsorption parameters. J Mol Liq 279:530–539. https://doi.org/10.1016/J.MOLLIQ.2019.01.162
2. Al-Ghouti MA, Al-Absi RS (2020) Mechanistic understanding of the adsorption and thermodynamic aspects of cationic methylene blue dye onto cellulosic olive stones biomass from wastewater. Sci Rep 10:15928. https://doi.org/10.1038/s41598-020-72996-3
3. Alimadadi M, Uesaka T (2016) 3D-oriented fiber networks made by foam forming. Cellulose 23:661–671
4. Allouss D, Essamlali Y, Amadine O et al (2019) Response surface methodology for optimization of methylene blue adsorption onto carboxymethyl cellulose-based hydrogel beads: Adsorption kinetics, isotherm, thermodynamics and reusability studies. RSC Adv 9:37858–37869. https://doi.org/10.1039/c9ra06450h
5. Amanullah M, Viswanathan S, Farooq S (2000) Equilibrium, kinetics, and column dynamics of methyl ethyl ketone biodegradation. Ind Eng Chem Res 39:3387–3396
6. Asim N, Badiei M, Alghoul MA et al (2019) Biomass and Industrial Wastes as Resource Materials for Aerogel Preparation: Opportunities, Challenges, and Research Directions. Ind Eng Chem Res 58:17621–17645. https://doi.org/10.1021/acs.iecr.9b02661
7. Azha SF, Shahadat M, Ismail S (2017) Acrylic polymer emulsion supported bentonite clay coating for the analysis of industrial dye. Dye Pigment 145:550–560. https://doi.org/10.1016/J.DYEPIG.2017.05.009

8. Bée A, Obeid L, Mbolantenaina R et al (2017) Magnetic chitosan/clay beads: A magsorbent for the removal of cationic dye from water. J Magn Magn Mater 421:59–64. https://doi.org/10.1016/J.JMMM.2016.07.022
9. Bhatti HN, Hayat J, Iqbal M et al (2018) Biocomposite application for the phosphate ions removal in aqueous medium. J Mater Res Technol 7:300–307. https://doi.org/10.1016/J.JMRT.2017.08.010
10. Bhatti HN, Safa Y, Yakout SM et al (2020) Efficient removal of dyes using carboxymethyl cellulose/alginate/polyvinyl alcohol/rice husk composite: Adsorption/desorption, kinetics and recycling studies. Int J Biol Macromol 150:861–870. https://doi.org/10.1016/j.ijbiomac.2020.02.093
11. Boukhalfa N, Boutahala M, Djebri N, Idris A (2019) Maghemite/alginate/functionalized multiwalled carbon nanotubes beads for methylene blue removal: Adsorption and desorption studies. J Mol Liq 275:431–440. https://doi.org/10.1016/J.MOLLIQ.2018.11.064
12. Cernencu AI, Lungu A, Dragusin D et al (2017) Design of cellulose–alginate films using PEG/NaOH aqueous solution as co-solvent. Cellulose 24:4419–4431. https://doi.org/10.1007/s10570-017-1412-9
13. Dąbrowski A (2001) Adsorption—from theory to practice. Adv Colloid Interface Sci 93:135–224
14. Dali Youcef L, Belaroui LS, López-Galindo A (2019) Adsorption of a cationic methylene blue dye on an Algerian palygorskite. Appl Clay Sci 179:105145. https://doi.org/https://doi.org/10.1016/j.clay.2019.105145
15. Eltaweil AS, Ali Mohamed H, Abd El-Monaem EM, El-Subruiti GM (2020a) Mesoporous magnetic biochar composite for enhanced adsorption of malachite green dye: Characterization, adsorption kinetics, thermodynamics and isotherms. Adv Powder Technol 31:1253–1263. https://doi.org/10.1016/J.APT.2020.01.005
16. Eltaweil AS, Elgarhy GS, El-Subruiti GM, Omer AM (2020b) Carboxymethyl cellulose/carboxylated graphene oxide composite microbeads for efficient adsorption of cationic methylene blue dye. Int J Biol Macromol 154:307–318. https://doi.org/10.1016/J.IJBIOMAC.2020.03.122
17. Feng C, Ren P, Huo M et al (2020) Facile synthesis of trimethylammonium grafted cellulose foams with high capacity for selective adsorption of anionic dyes from water. Carbohydr Polym 241:116369. https://doi.org/10.1016/J.CARBPOL.2020.116369
18. Franco P, Cardea S, Tabernero A, De Marco I (2021) Porous Aerogels and Adsorption of Pollutants from Water and Air: A Review. Mol. 26
19. Ge X, Wu Z, Cravotto G et al (2018) Cork wastewater purification in a cooperative flocculation/adsorption process with microwave-regenerated activated carbon. J Hazard Mater 360:412–419. https://doi.org/10.1016/J.JHAZMAT.2018.08.022
20. Hasanzadeh M, Simchi A, Shahriyari Far H (2020) Nanoporous composites of activated carbon-metal organic frameworks for organic dye adsorption: Synthesis, adsorption mechanism and kinetics studies. J Ind Eng Chem 81:405–414. https://doi.org/https://doi.org/10.1016/j.jiec.2019.09.031

21. Hjelt T, Kinnunen K, Lehmonen J et al (2011) Intriguing structural and strength behavior in foam forming. na
22. Ho YS, Ng JCY, McKay G (2000) Kinetics of pollutant sorption by biosorbents. Sep Purif methods 29:189–232
23. Hou Q, Wang X (2017) The effect of PVA foaming characteristics on foam forming. Cellulose 24:4939–4948
24. Hu Z, Cai L, Liang J et al (2019) Green synthesis of expanded graphite/layered double hydroxides nanocomposites and their application in adsorption removal of Cr(VI) from aqueous solution. J Clean Prod 209:1216–1227. https://doi.org/10.1016/J.JCLEPRO.2018.10.295
25. Huang Z, Li Y, Chen W et al (2017) Modified bentonite adsorption of organic pollutants of dye wastewater. Mater Chem Phys 202:266–276. https://doi.org/https://doi.org/10.1016/j.matchemphys.2017.09.028
26. Jiang L, Zhang Y, Zhou M et al (2018) Oxidation of Rhodamine B by persulfate activated with porous carbon aerogel through a non-radical mechanism. J Hazard Mater 358:53–61. https://doi.org/10.1016/J.JHAZMAT.2018.06.048
27. Kalia S, Dufresne A, Cherian BM et al (2011) Cellulose-based bio- and nanocomposites: A review.Int. J. Polym. Sci
28. Karami D (2018) A review of aerogel applications in adsorption and catalysis. J Pet Sci Technol 8:3–15
29. Lakouraj MM, Norouzian R-S, Balo S (2015) Preparation and Cationic Dye Adsorption of Novel Fe3O4 Supermagnetic/Thiacalix[4]arene Tetrasulfonate Self-Doped/Polyaniline Nanocomposite: Kinetics, Isotherms, and Thermodynamic Study. J Chem Eng Data 60:2262–2272. https://doi.org/10.1021/acs.jced.5b00080
30. Lavoine N, Desloges I, Dufresne A, Bras J (2012) Microfibrillated cellulose - Its barrier properties and applications in cellulosic materials: A review. Carbohydr Polym 90:735–764. https://doi.org/10.1016/j.carbpol.2012.05.026
31. Lee H, Kim S, Shin S, Hyun J (2021) 3D structure of lightweight, conductive cellulose nanofiber foam. Carbohydr Polym 253:117238. https://doi.org/10.1016/J.CARBPOL.2020.117238
32. Li J, Li H, Yuan Z et al (2019) Role of sulfonation in lignin-based material for adsorption removal of cationic dyes. Int J Biol Macromol 135:1171–1181. https://doi.org/10.1016/J.IJBIOMAC.2019.06.024
33. Li X, Li Y, Zhang S, Ye Z (2012) Preparation and characterization of new foam adsorbents of poly(vinyl alcohol)/chitosan composites and their removal for dye and heavy metal from aqueous solution. Chem Eng J 183:88–97. https://doi.org/10.1016/J.CEJ.2011.12.025
34. Liu P, Zhu C, Mathew AP (2019) Mechanically robust high flux graphene oxide - nanocellulose membranes for dye removal from water. J Hazard Mater 371:484–493. https://doi.org/10.1016/J.JHAZMAT.2019.03.009

35. Liu Y, Kong S, Xiao H et al (2018) Comparative study of ultra-lightweight pulp foams obtained from various fibers and reinforced by MFC. Carbohydr Polym 182:92–97
36. Lu B, Lin Q, Yin Z et al (2021) Robust and lightweight biofoam based on cellulose nanofibrils for high-efficient methylene blue adsorption. Cellulose 28:273–288
37. Ma H, Zhang XF, Wang Z et al (2021) Flexible cellulose foams with a high loading of attapulgite nanorods for Cu2 + ions removal. Colloids Surf Physicochem Eng Asp 612:126038. https://doi.org/10.1016/J.COLSURFA.2020.126038
38. Oz M, Lorke DE, Hasan M, Petroianu GA (2011) Cellular and molecular actions of Methylene Blue in the nervous system. Med Res Rev 31:93–117. https://doi.org/https://doi.org/10.1002/med.20177
39. Premarathna KSD, Rajapaksha AU, Sarkar B et al (2019) Biochar-based engineered composites for sorptive decontamination of water: A review. Chem Eng J 372:536–550
40. Qi X, Wei W, Su T et al (2018) Fabrication of a new polysaccharide-based adsorbent for water purification. Carbohydr Polym 195:368–377. https://doi.org/10.1016/J.CARBPOL.2018.04.112
41. Radwan EK, El-Naggar ME, Abdel-Karim A, Wassel AR (2021) Multifunctional 3D cationic starch/nanofibrillated cellulose/silver nanoparticles nanocomposite cryogel: Synthesis, adsorption, and antibacterial characteristics. Int J Biol Macromol 189:420–431. https://doi.org/10.1016/J.IJBIOMAC.2021.08.108
42. Sabarish R, Unnikrishnan G (2018) Polyvinyl alcohol/carboxymethyl cellulose/ZSM-5 zeolite biocomposite membranes for dye adsorption applications. Carbohydr Polym 199:129–140. https://doi.org/10.1016/J.CARBPOL.2018.06.123
43. Simonin JP (2016) On the comparison of pseudo-first order and pseudo-second order rate laws in the modeling of adsorption kinetics. Chem Eng J 300:254–263. https://doi.org/10.1016/J.CEJ.2016.04.079
44. Somsesta N, Sricharoenchaikul V, Aht-Ong D (2020) Adsorption removal of methylene blue onto activated carbon/cellulose biocomposite films: Equilibrium and kinetic studies. Mater Chem Phys 240:122221. https://doi.org/10.1016/J.MATCHEMPHYS.2019.122221
45. Song K, Zhu W, Li X, Yu Z (2020) A novel mechanical robust, self-healing and shape memory hydrogel based on PVA reinforced by cellulose nanocrystal. Mater Lett 260:126884. https://doi.org/10.1016/J.MATLET.2019.126884
46. Sonker AK, Rathore K, Nagarale RK, Verma V (2018) Crosslinking of Polyvinyl Alcohol (PVA) and Effect of Crosslinker Shape (Aliphatic and Aromatic) Thereof. J Polym Environ 26:1782–1794. https://doi.org/10.1007/s10924-017-1077-3
47. Tan KL, Hameed BH (2017) Insight into the adsorption kinetics models for the removal of contaminants from aqueous solutions. J Taiwan Inst Chem Eng 74:25–48. https://doi.org/10.1016/J.JTICE.2017.01.024
48. Tan X, Peng Q, Yang K et al (2021) Preparation and Characterization of corn husk nanocellulose coating on electrospun polyamide 6. Alexandria Eng J. https://doi.org/10.1016/J.AEJ.2021.10.011

49. Tang S, Xia D, Yao Y et al (2019) Dye adsorption by self-recoverable, adjustable amphiphilic graphene aerogel. J Colloid Interface Sci 554:682–691. https://doi.org/10.1016/J.JCIS.2019.07.041
50. Tucker IM, Petkov JT, Penfold J, Thomas RK (2012) Interaction of the anionic surfactant SDS with a cellulose thin film and the role of electrolyte and poyelectrolyte. 2 Hydrophilic cellulose. Langmuir 28:10223–10229
51. Usmani Z, Sharma M, Awasthi AK et al (2021) Bioprocessing of waste biomass for sustainable product development and minimizing environmental impact. Bioresour Technol 322:124548
52. Verma A, Thakur S, Mamba G et al (2020) Graphite modified sodium alginate hydrogel composite for efficient removal of malachite green dye. Int J Biol Macromol 148:1130–1139. https://doi.org/10.1016/J.IJBIOMAC.2020.01.142
53. Viitala J, Lappalainen T, Järvinen M (2020) Sodium dodecyl sulphate (SDS) residue analysis of foam-formed cellulose-based products. Nord Pulp Pap Res J 35:261–271
54. Wang J, Guo X (2020a) Adsorption kinetic models: Physical meanings, applications, and solving methods. J Hazard Mater 390:122156. https://doi.org/10.1016/J.JHAZMAT.2020.122156
55. Wang J, Guo X (2020b) Adsorption isotherm models: Classification, physical meaning, application and solving method. Chemosphere 258:127279. https://doi.org/10.1016/J.CHEMOSPHERE.2020.127279
56. Wang S, Ning H, Hu N et al (2019) Preparation and characterization of graphene oxide/silk fibroin hybrid aerogel for dye and heavy metal adsorption. Compos Part B Eng 163:716–722. https://doi.org/10.1016/J.COMPOSITESB.2018.12.140
57. Wang Y, Zhao L, Hou J et al (2018) Kinetic, isotherm, and thermodynamic studies of the adsorption of dyes from aqueous solution by cellulose-based adsorbents. Water Sci Technol 77:2699–2708. https://doi.org/10.2166/wst.2018.229
58. Weaire D, Phelan R (1996) The physics of foam. J Phys Condens Matter 8:9519
59. Yan Zhijuan Gao LA Dissolving of cellulose in PEG/NaOH aqueous solution. https://doi.org/10.1007/s10570-008-9233-5
60. Yang L, Zhan Y, Gong Y et al (2021) Development of eco-friendly CO2-responsive cellulose nanofibril aerogels as “green” adsorbents for anionic dyes removal. J Hazard Mater 405:124194. https://doi.org/10.1016/J.JHAZMAT.2020.124194

Figures

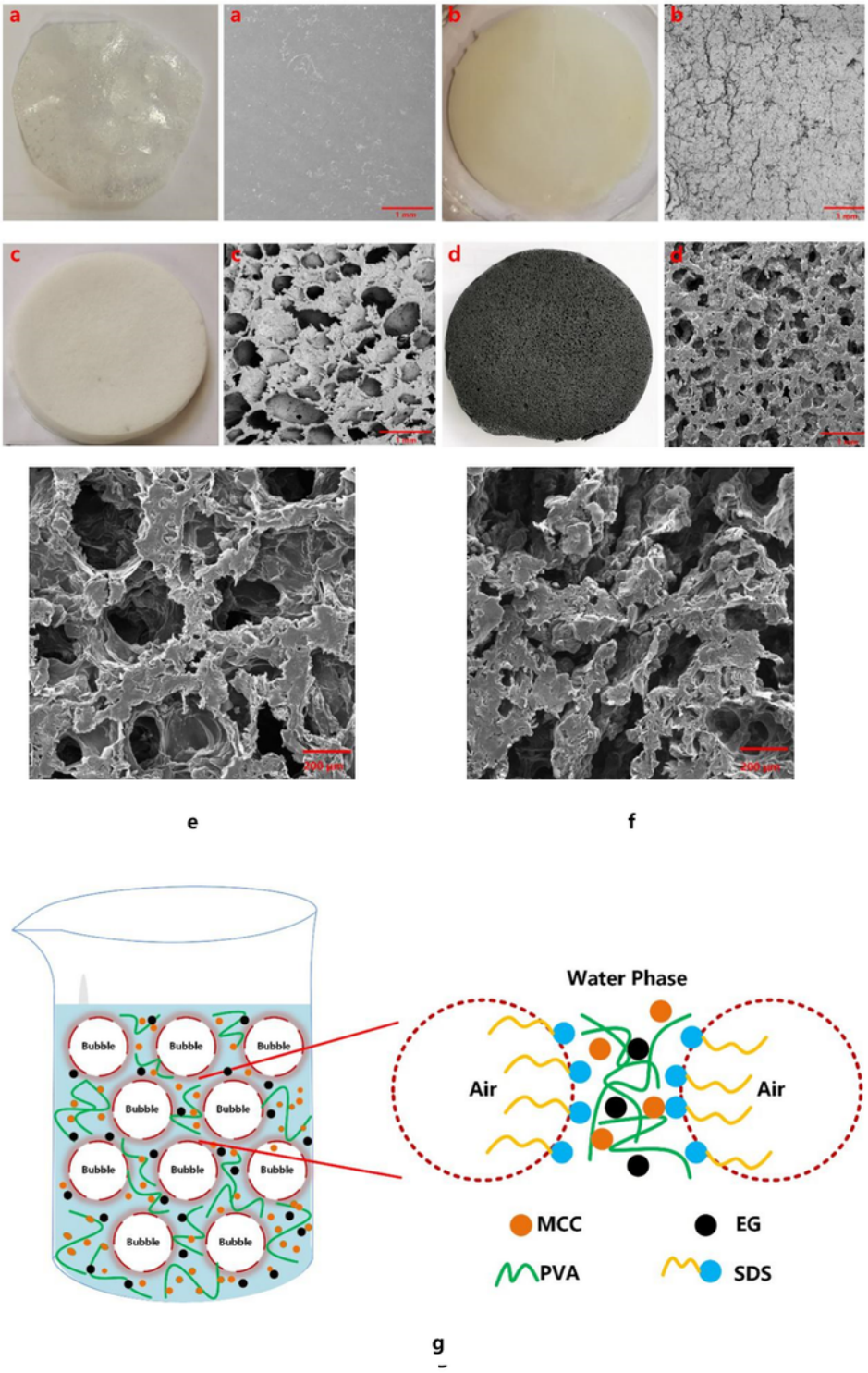

Figure 1

Surface morphology. (a: PS; b: CP; c: CPS; d: CPSG; e: front side of CPSG; f: cross-section of CPSG; g: schematic diagram)

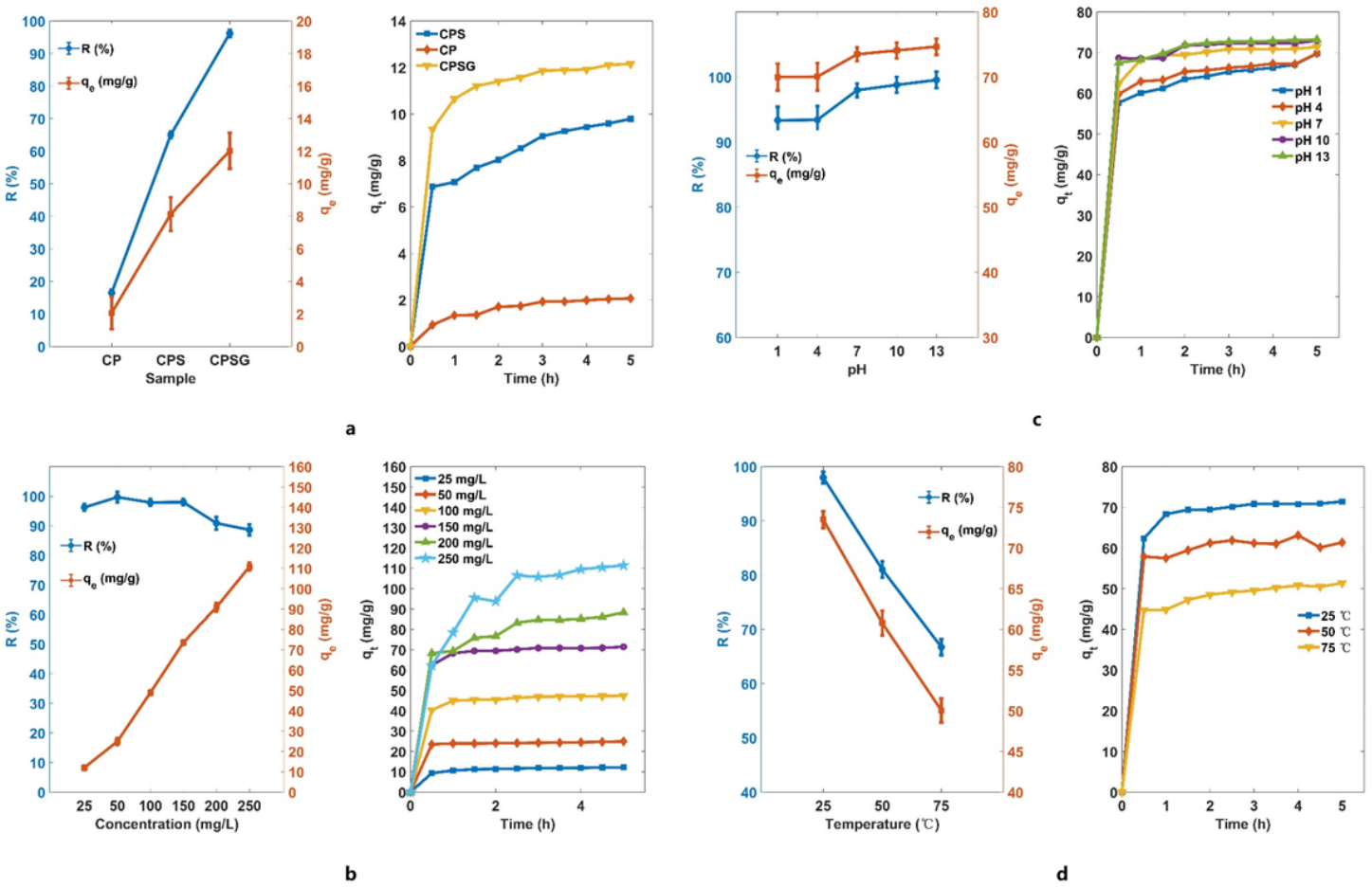

Figure 2

a: The influence of CP, CPS, and CPSG on adsorption, b: The effect of different initial concentrations of dyes on adsorption, The influence of different pH values on adsorption, d: The effect of temperature on adsorption.

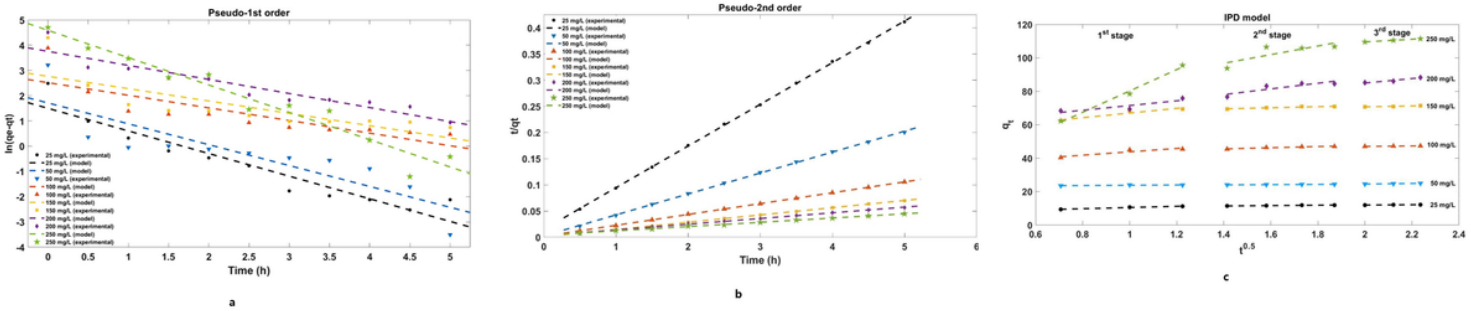

Figure 3

Adsorption kinetic models. a: Pseudo-1st order; b: Pseudo-2nd order; c: IPD model.

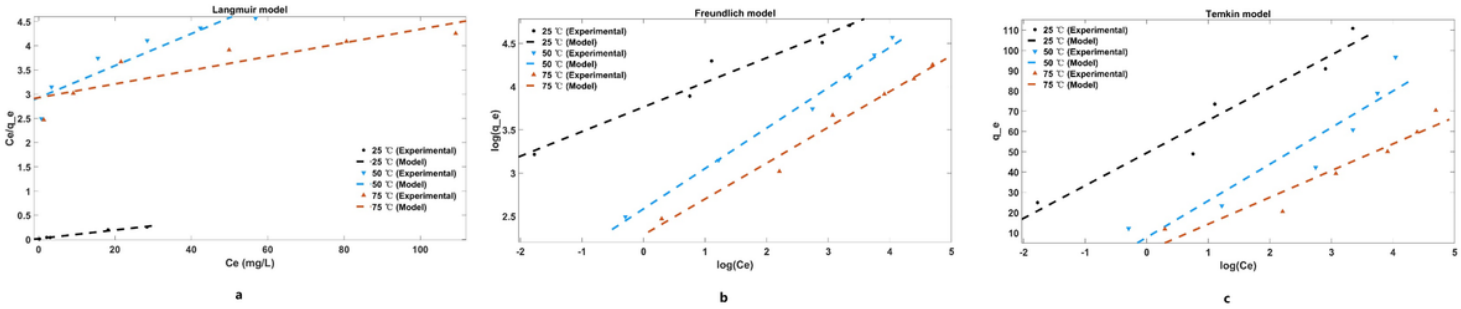

Figure 4

Adsorption isotherm models. a: Langmuir model; b: Freundlich model; c: Temkin model.

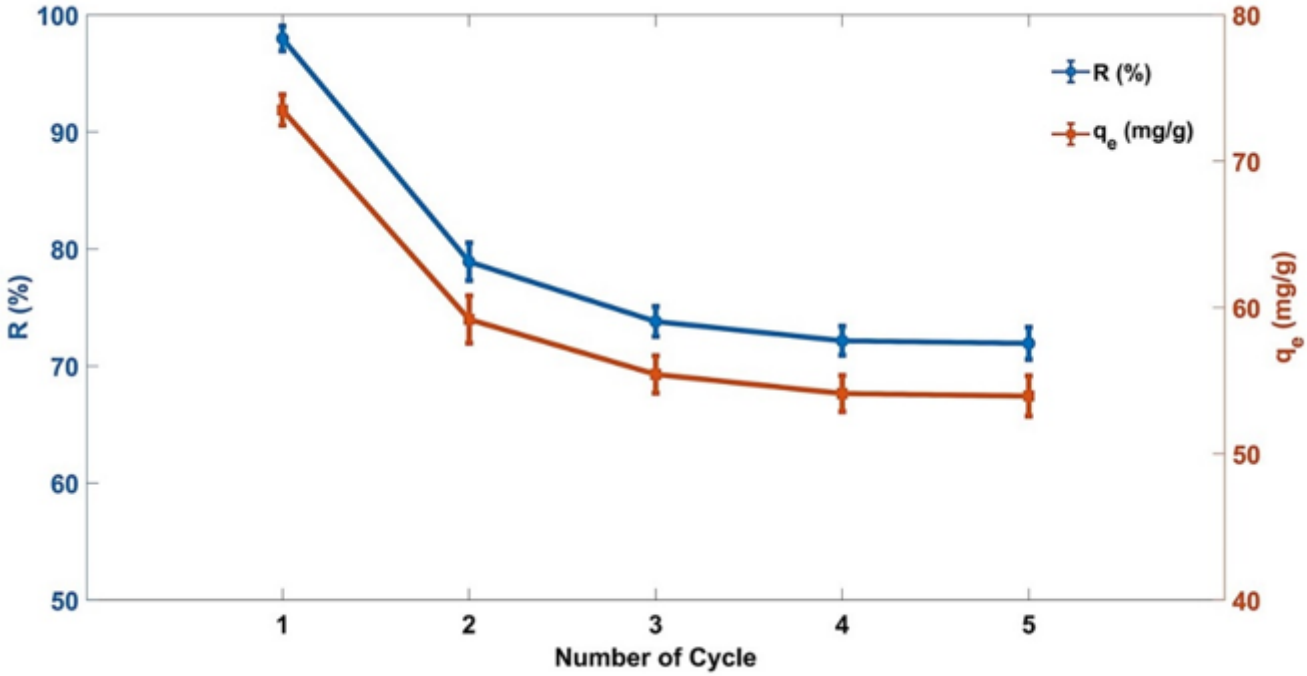

Figure 5

Reusability of porous foam composites in MB adsorption.

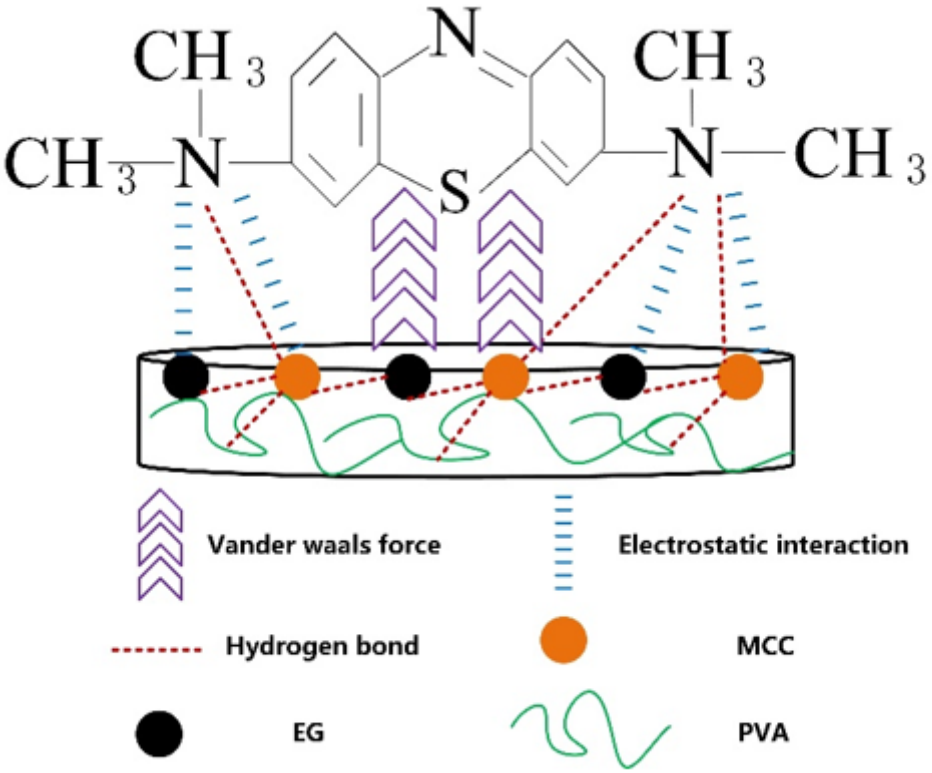

Figure 6

Possible interaction mechanism between cellulose-based porous foam material and MB molecule.

Supplementary Files

This is a list of supplementary files associated with this preprint. Click to download.

- SupportInformation.docx